Biochimica et Biophysica Acta, 1065 (1991) 177–184

ADONIS 000527369100241X

BBAMEM 75260

Quantification of Ca^{2+}-ATPases in porcine duodenum. Effects of $1,25(OH)_2D_3$ deficiency

J.A.H. Timmermans, R. Kaune *, R.J.M. Bindels and C.H. van Os

Department of Physiology, University of Nijmegen, Nijmegen (The Netherlands)

(Received 14 December 1990)

Key words: ATPase, Ca^{2+}-; Calcium ion transport; Basolateral membrane; (Pig)

Previous studies have identified a calmodulin-stimulated ATP-dependent Ca^{2+} pump as the major Ca^{2+} efflux pathway in enterocytes. Here, we developed methods to quantify the number of Ca^{2+} pumps in basolateral and intracellular membranes from porcine duodenum. By the use of a pig strain with a genetic defect in renal 1α-hydroxylase, we were able to investigate the influence of $1,25(OH)_2D_3$-deficiency on the number of Ca^{2+}-ATPases in porcine duodenum. The amount of Ca^{2+}-ATPase in isolated basolateral membranes was 5.5 ± 0.7 μg/mg protein, while the V_{max} of ATP-dependent Ca^{2+} transport into inside-out resealed basolateral membrane vesicles was 2.6 ± 0.4 nmol/mg protein per min. From these data we estimated roughly about $95 \cdot 10^3$ plasma membrane Ca^{2+} pump sites per enterocyte. In addition, the amount of intracellular Ca^{2+}-ATPase in microsomal fractions was 0.41 ± 0.02 μg/mg protein. Comparison of these parameters between control and rachitic animals showed that Ca^{2+} pump capacities in both basolateral membranes and microsomal fractions of porcine duodenum are not influenced by $1,25(OH)_2D_3$-deficiency. In conclusion, stimulatory effects of $1,25(OH)_2D_3$ on intestinal Ca^{2+} transport most likely result from specific effects on apical influx and facilitation of cytosolic Ca^{2+} diffusion by Ca^{2+}-binding proteins and not from an increase in Ca^{2+} pumping capacity in basolateral membranes.

Introduction

Net calcium absorption in the intestine is the result of passive and active transport mechanisms. Passive Ca^{2+} absorption and/or secretion via the paracellular pathway occurs along the whole small intestine, while active transcellular absorption is restricted to the proximal small intestine [1]. Active absorption is dependent on the level of circulating $1,25(OH)_2D_3$ and consists of Ca^{2+} influx via the brush border, diffusion of Ca^{2+} through the cytosol and active extrusion via the basolateral membrane. Studies of Ca^{2+} uptake into inside-out-orientated basolateral membrane vesicles have demonstrated a calmodulin-stimulated ATP-dependent Ca^{2+} pump as the predominant Ca^{2+} transport system in mammalian small intestine [2–6]. Since Ca^{2+}-ATPases comprise only a minor fraction of the plasma membrane proteins, the identification and quantification of Ca^{2+} pumps in epithelial cells is difficult. For example, (i) Ca^{2+}-dependent ATPase activities were markedly different from ATP-driven Ca^{2+} uptake rates in basolateral membrane vesicles [7–9], (ii) ATP-dependent Ca^{2+} uptake activity is only present in resealed, inside-out vesicles which constitute a minor fraction of basolateral membrane preparations, (iii) ATP-driven Ca^{2+} uptake activity in duodenal basolateral vesicles of vitamin D-deficient rats may be inactivated during isolation of enterocytes [10].

Besides a calmodulin-dependent Ca^{2+} pump in the basolateral membrane, enterocytes contain intracellular Ca^{2+} pumps with similar properties as the one

* Permanent address: Institute of Physiology, School of Veterinary Medicine, Hannover, Germany.

Abbreviations: BSA, bovine serum albumin; EGTA, ethylene glycol bis(β-aminoethyl ether)-*N*,*N*'-tetraacetic acid; ELISA, enzyme-linked immunosorbent assay; HEEDTA, *N*-(2-hydroxyethyl)ethylenediamine-*N*,*N*',*N*'-triacetic acid; Hepes, 4-(2-hydroxyethyl)-1-piperazineethanesulphonic acid; imidazole, 1,3-diaza-2,4-cyclopentadiene; NTA, nitrilotriacetic acid; PMSF, phenylmethanesulphonyl fluoride; SDS-PAGE, sodium dodecyl sulphate polyacrylamide gel electrophoresis; TCA, trichloroacetic acid; Tris, tris(hydroxymethyl) aminomethane.

Correspondence: C.H. Van Os, Department of Physiology, University of Nijmegen, P.O.Box 9101, 6500 HB Nijmegen, The Netherlands.

from sarcoplasmic reticulum [11–13]. Quantification of intracellular Ca^{2+}-ATPase in enterocytes proved difficult for similar reasons as given above [14].

In the present study, we developed competitive ELISAs for both Ca^{2+}-ATPases and were able to quantify the number of Ca^{2+} pumps in porcine duodenal epithelium. By the use of piglets with pseudo vitamin D-deficiency rickets type I, a pig strain with an inherited defect in renal 1α-hydroxylase [15], the influence of $1,25(OH)_2D_3$-deficiency on the number of Ca^{2+} pumps was studied.

Materials and Methods

Animals

Eight homozygote piglets with pseudo vitamin D-deficiency rickets, type 1 ('Hannover Pig Strain') and seven clinically normal heterozygote litter mates were used. The piglets belonged to four different litters, and were 50–60 days old, with body weights between 3.8 and 13.4 kg. The plasma calcium levels in control animals were between 2.68 and 3.27 mM, and in the rachitic piglets between 1.28 and 2.48 mM. The activity of plasma alkaline phosphatase ranged from 159 to 334 U/l (control) and from 893 to 1907 U/l (rachitic). After a weaning period to an age of 30–40 days, the piglets were fed a diet containing 0.8% calcium, 0.6% phosphorus and 37.5 μg (1500 U) vitamin D/kg. The animals were killed by stunning and bled from the dissected carotid arteries. Immediately after bleeding, the duodenum (proximal 20–30 cm of the small intestine) was removed, flushed with cold isotonic saline and frozen in liquid nitrogen. The frozen intestine were stored at −80°C.

Preparation of basolateral membranes

In each experiment, membranes were prepared simultaneously from a rachitic and from a control piglet. Basolateral membranes were prepared from mucosal scrapings, according to Ghijsen et al. [8]. About 0.6–0.7 g wet weight of mucosal scrapings were vortexed with 30 ml saline and centrifuged at $200 \times g$ for 10 min. The pellet was homogenised for 1 min with a polytron (Braun) in 15 ml of 25 mM NaCl, 1 mM Hepes-Tris (pH 8.0), diluted with the same medium to 50 ml and centrifuged at $600 \times g$ for 10 min. The supernatant was centrifuged at $100000 \times g$ for 20 min. The resulting pellet was resuspended in about 6 ml medium containing 250 mM sucrose, 5 mM $MgCl_2$ and 10 mM Hepes-Tris (pH 7.4) in a Dounce apparatus by 100 strokes with a loose-fitting pestle. The suspension was brought to 40% sorbitol concentration by the addition of 60% (w/v) sorbitol solution (containing 10 mM Hepes-Tris, pH 7.4) and centrifuged at $200000 \times g$ for 1.5 h in a swing-out rotor. The membranes positioned between the 40% sucrose layer and the overlay buffer were removed with a syringe, mixed with the final uptake medium (150 mM KCl, 1 mM $MgCl_2$, 20 mM Hepes-Tris, pH 7.4) and centrifuged at $100000 \times g$ for 20 min. The final pellet was resuspended in uptake medium. All steps of the preparation were carried out at 0–4°C with 1 mM dithiothreitol and 0.4 mM PMSF added to the homogenisation and sorbitol buffers.

Preparation of microsomal membranes

To prepare a microsomal fraction, the scrapings were vortexed with saline and centrifuged as described above. The pellets were homogenised in a medium containing 250 mM sucrose, 0.5 mM EGTA, 3 mM Hepes-KOH, 1 mM dithiothreitol and 0.4 mM PMSF (pH 7.4). The suspension was homogenised in a Dounce apparatus, first with 4–6 strokes of a loose-fitting pestle, then with 10–15 strokes of a tight-fitting pestle. After centrifugation at $10000 \times g$ for 10 min, the supernatant was centrifuged at $100000 \times g$ for 60 min and the pellet was resuspended in uptake medium.

Determination of Ca^{2+} uptake in the vesicles

Ca^{2+} uptake studies were done at 37°C by a rapid filtration technique as described previously [4,12]. The uptake medium for basolateral membranes contained 150 mM KCl, 0.5 mM EGTA, 0.5 mM HEEDTA, 20 mM Hepes-Tris adjusted to pH 7.2. The free Mg^{2+} concentration was adjusted to 1.5 mM by adding $MgCl_2$, and the free Ca^{2+} between 0.01 and 5.0 μM by adding $CaCl_2$ in amounts calculated according to a routine described by Van Heeswijk et al. [16]. ATP was added as Tris-ATP to a final concentration of 3 mM. The uptake medium for microsomes contained 120 mM KCl, 20 mM sodium oxalate when indicated, 1.2 mM KH_2HPO_4, 5 mM pyruvate, 5 mM succinate, 0.5 mM EGTA, 0.5 mM HEEDTA, 20 mM Hepes-KOH, 0.05% BSA, 10 mM creatinine phosphate and 10 U/ml creatinine kinase (pH 7.2). The free Mg^{2+} was adjusted to 1.5 mM, the free Ca^{2+} to 1 μM, and ATP was added as Mg-ATP to a final concentration of 10 mM.

^{125}I-calmodulin overlay

Membrane protein was applied to a 7.5–15% gradient polyacrylamide gel according to Leammli et al. [17]. The proteins were transferred to nitrocellulose sheets and blocked with excess BSA. Subsequently, the sheets were incubated for 45 min in a medium containing 20 mM Tris-HCl, 150 mM NaCl, 0.1 mM $CaCl_2$, 0.5% BSA (pH 7.4) and about 0.15 nmol ^{125}I-calmodulin (spec. act. 0.74 MBq/nmol). After washing three times, the blot was dried, marked with radioactive ink, and exposed to Kodak X-Omat film at −80°C. The radioactive band corresponding to the Ca^{2+} pump was cut out and counted in a multigamma counter (LKB). Calmodulin was isolated from bovine brain according

to Gopalakrishna [18]. Iodination of calmodulin was performed as described by Bolton and Hunter [19].

Competitive ELISAs for Ca^{2+}-ATPases

Ca^{2+}-ATPase from pig erythrocytes was isolated according to Niggli et al. [20]. Ca^{2+}-ATPase from rat skeletal muscle sarcoplasmic reticulum was isolated with DEAE-chromatography after solubilisation of membrane proteins, essentially as described by Heilman [21]. The Ca^{2+}-ATPase was eluted at 100 mM NaCl. 40 μg purified Ca^{2+}-ATPase in Freund's complete adjuvans was injected into rabbits. Each week, the animals were boosted with the same amount of antigen in Freund's incomplete adjuvans. After 6 weeks, the animals were killed and bled. A competitive ELISA was developed in the following way: (i) 50 ng purified Ca^{2+}-ATPase were coated to each well of a polystyrene plate, in a total volume of 100 μl coating buffer, containing 0.1 M Na_2CO_3 and 5 mM NaN_3 (pH 9.6), for 2 h at 37°C; (ii) 50 μl samples of purified Ca^{2+}-ATPase or solubilised test samples were added to each well, followed by 50 μl antiserum. The plate was incubated overnight at 4°C to reach equilibrium; (iii) 100 μl/well peroxidase-labelled goat anti-rabbit IgGs (1:500) were added and incubated for 2 h at 20°C. Colour was developed by adding 100 μl medium containing 0.5 mg/ml *o*-phenyldiamine in 23 mM citric acid, 66 mM NaH_2PO_4 and 0.01% H_2O_2 (pH 5.5). The reaction was terminated by adding 100 μl/well 2 M H_2SO_4 and after 5 min the absorbance was determined in an EIA-reader (Bio-Rad). Antisera and antigen were diluted in 10 mM Tris-HCl, 0.9% NaCl, 0.05% Tween-20 and 0.5% BSA (pH 7.4). Following each step, the ELISA plate was washed four times for 2 min with 10 mM Tris-HCl, 0.9% NaCl and 0.05% Tween-20 (pH 7.4). Duodenal microsomes and standard samples were brought to a concentration of ± 3 mg/ml and mixed with an equal volume of solubilisation buffer (130 mM KCl, 20 mM Hepes-Tris, 1 mM $MgCl_2$, 50 μM $CaCl_2$ and 0.4% Triton X-100 (pH 7.4)) for 15 min at room temperature. After centrifugation at $100000 \times g$ for 5 min in a Beckman airfuge, the supernatants were applied to the ELISA plate.

Immunoblotting

Membrane protein was applied to a 10% SDS-PAGE, according to Laemmli et al. [17] and run in a mini-gel apparatus (Bio-Rad). Subsequently, the proteins were transferred to nitrocellulose sheets and incubated overnight at room temperature in 10 mM Tris-HCl, 0.9% NaCl, 0.05% Tween-20 and 1% BSA (pH 7.4). The blot was incubated, firstly, with antiserum (anti-red blood cell 1:300; anti-SR 1:750) in the same buffer for 2 h at room temperature, and secondly, with peroxidase-labelled goat anti-rabbit IgG(H&L) (1:500) for 2 h at room temperature in the same buffer. Colour was developed by incubation with 0.5 mg/ml 4-chloronaphthol in 15% methanol, 10 mM Tris-HCl, 0.9% NaCl and 0.01% H_2O_2 (pH 7.4).

Enzyme assays

Na^+/K^+-ATPase, succinate dehydrogenase (SDH), alkaline phosphatase (AP) and NADPH–cytochrome-*c* reductase activities were determined, as previously described [12]. The orientation of the basolateral vesicles was determined by measuring the Na^+/K^+-ATPase activity in the absence and presence of 0.5 μg digitonin per mg protein and 0.1 mM ouabain for 15 min at 37°C. Medium containing digitonin gives the total Na^+/K^+-ATPase activity. Na^+/K^+-ATPase in inside-out orientated vesicles is not ouabain-sensitive within short incubation periods (up to 15 min), since ouabain penetration into the vesicle is slow. The basolateral membrane preparation contains $15 \pm 3\%$ ($n = 4$) inside-out resealed vesicles. Protein was determined with the Coomassie blue method (Bio-Rad) in the presence of 0.1% Triton X-100, using bovine γ-globulin as standard.

Data are presented as the mean $\pm$ S.E. and statistical significance was tested using Student's *t*-tests.

Chemicals

EGTA, NTA, HEEDTA, Tris-ATP, Mg-ATP, PMSF, β-glycerophosphate and peroxidase-labelled goat anti-rabbit IgG (H&L) were obtained from Sigma (St. Louis). $^{45}CaCl_2$ and ^{125}I were purchased from New England Nuclear (Dreieich, Germany), [γ-^{32}P]ATP from Radiochemical Centre (Amersham, U.K.), ruthenium red from Merck (Darmstadt, Germany), and sodium orthovanadate from ICN (Plain View, NY, U.S.A.). Bithiothreitol, calcium ionophore A23187 and calf intestinal alkaline phosphatase were purchased from Boehringer (Mannheim, Germany). All other chemicals were of the purest grade.

Results

Immunology and calmodulin binding

Basolateral membrane vesicles from pig enterocytes were purified 5-fold in Na^+/K^+-ATPase activity. The microsomal vesicles were purified 3-fold with respect to NADPH–cytochrome-*c* reductase. No differences in purification factors between duodenal preparations from rachitic and control piglets were observed (Table I).

Although Ca^{2+}-ATPase in basolateral membranes is calmodulin-dependent, attempts to purify this Ca^{2+}-pump using calmodulin-affinity chromatography were unsuccessful. Calmodulin depletion of the membrane fraction before solubilisation is a prerequisite for calmodulin-affinity chromatography, but the abundantly-present, and tightly-bound calmodulin in intesti-

TABLE I

Enrichment factors for marker enzymes in basolateral and microsomal membranes from control and rachitic piglets

Values are the means ±S.E. for five animals. Control and rachitic animal preparations are not significantly different (all P values > 0.05).

	Na^+/K^+ ATPase	Succinate dehydrogenase	Alkaline phosphatase	NADPH–cyt.-*c* reductase
Basolateral				
control	4.9±0.6	1.0±0.1	2.6±0.4	1.6±0.3
rachitic	5.7±0.5	0.8±0.2	2.4±0.4	1.3±0.2
Microsomal				
control	1.5±0.3	0.3±0.1	1.3±0.3	3.5±0.6
rachitic	1.3±0.2	0.4±0.1	1.5±0.4	3.0±0.5

nal membrane fractions could not be removed with methods used to deplete Ca^{2+}-ATPase from red cells or heart plasmalemma [5,20]. Since purification of basolateral Ca^{2+}-ATPase was not possible, an indirect method for quantifying this pump was developed.

Firstly, polyclonal antibodies were raised against the purified Ca^{2+}-ATPase from pig red cell membranes and from rat sarcoplasmic reticulum. Both antibodies were specific for their own antigen illustrated in Figs. 1A and B by means of Western blotting. Using a competitive ELISA, it was shown that the antibodies against pig red cell Ca^{2+}-ATPase did not recognise the intestinal plasma membrane Ca^{2+}-ATPase (Figs. 2A and B). In contrast, antibodies against rat sarcoplasmic reticulum Ca^{2+}-ATPase exhibited good cross-reactivity with intestinal microsomal Ca^{2+}-ATPases (Figs. 3A

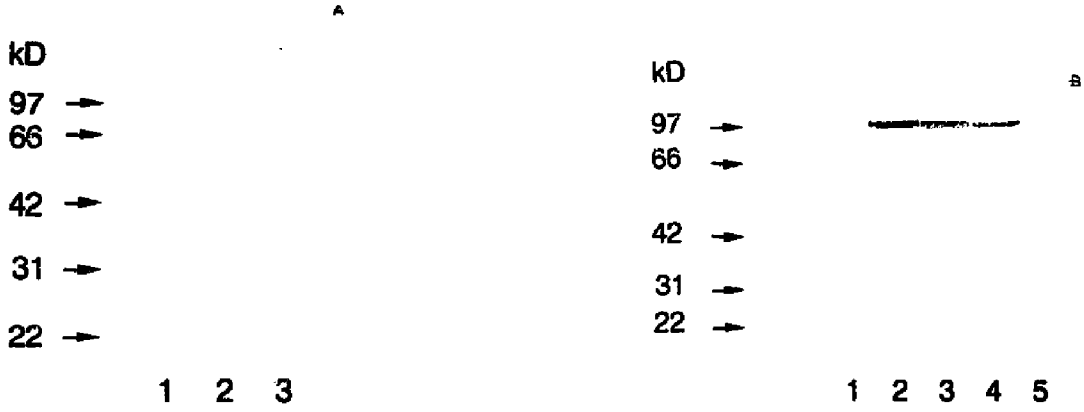

Fig. 1. Western blots of antisera against porcine erythrocyte Ca^{2+}-ATPase (A) and rat sarcoplasmic reticulum Ca^{2+}-ATPase (B). (A) Lane 1: 1 μg purified porcine erythrocyte Ca^{2+}-ATPase; lane 2: 25 μg porcine erythrocyte ghost; lane 3: 1 μg purified porcine sarcoplasmic reticulum Ca^{2+}-ATPase. The blots were incubated with 300×diluted antiserum against purified porcine erythrocyte Ca^{2+}-ATPase. (B) Lane 1: 1 μg purified porcine erythrocyte Ca^{2+}-ATPase; lane 2: 1 μg purified porcine sarcoplasmic reticulum Ca^{2+}-ATPase; lane 3: 1 μg purified rabbit sarcoplasmic reticulum Ca^{2+}-ATPase; lane 4: 1 μg purified rat sarcoplasmic reticulum Ca^{2+}-ATPase; lane 5: 2 μg purified rabbit renal Na^+/K^+-ATPase The blots were incubated with 750×diluted antiserum against purified rat sarcoplasmic reticulum Ca^{2+}-ATPase.

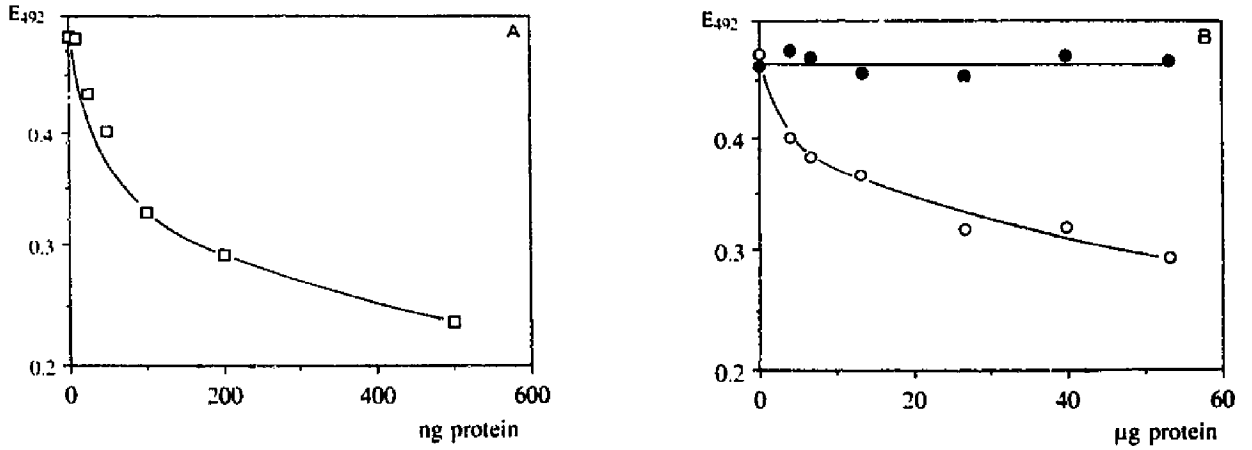

Fig. 2. (A) Competitive ELISA for purified porcine red cell Ca^{2+}-ATPase. Each well was coated with 50 ng purified porcine red cell Ca^{2+}-ATPase (see Methods for further details). (B) Competitive ELISA: Competition between 50 ng purified porcine red cell Ca^{2+}-ATPase and varying amounts of red cell ghost (○——○) or basolateral membranes from porcine duodenum epithelium (●——●) (see Methods for further details).

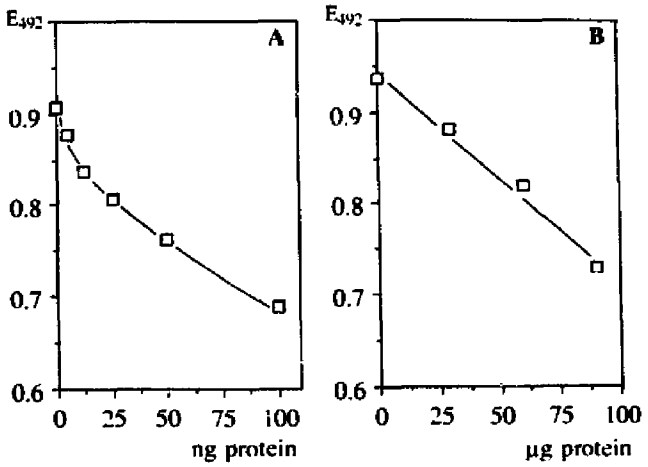

Fig. 3. (A) Competitive ELISA for purified rat sarcoplasmic reticulum Ca^{2+}-ATPase. Each well was coated with 50 ng purified Ca^{2+}-ATPase (see Methods for further details). (B) Competitive ELISA: Competition between 50 ng purified rat sarcoplasmic reticulum Ca^{2+}-ATPase and varying amounts of microsomes membranes from porcine duodenum (see Methods for further details).

and B). Secondly, with the ^{125}I-calmodulin overlay technique, a quantitative relationship between the amount of ghost protein or intestinal membrane protein and the radioactivity on blots could be obtained (Fig. 4). Hence, the amount of Ca^{2+}-ATPase in pig intestinal basolateral membranes can be expressed in equivalent pig ghosts. Using the competitive ELISA for pig ghost Ca^{2+}-ATPase, the equivalent pig ghosts can then be converted into the actual amount of Ca^{2+}-ATPase per mg basolateral membrane protein. The results of the ^{125}I-calmodulin overlay technique and the competitive ELISA for the basolateral Ca^{2+}-

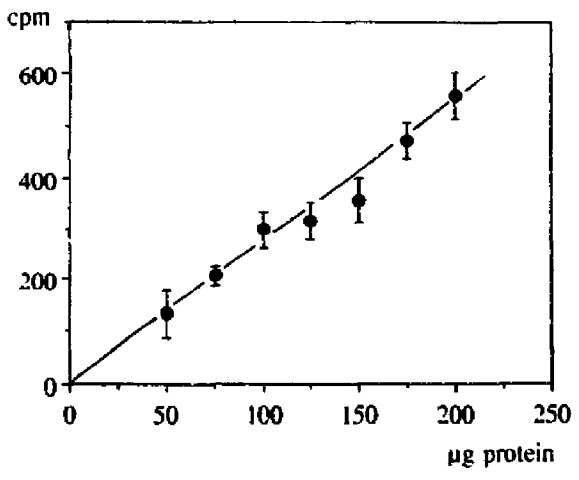

Fig. 4. Calibration curve for the ^{125}I-calmodulin overlay technique. Porcine red blood cell ghost is subjected to SDS-PAGE in increasing amounts and subsequently blotted onto nitrocellulose paper (x-axis). After incubation with ^{125}I-calmodulin and after washing, bound ^{125}I-calmodulin is counted (y-axis). Linear regression yields: $y = 2.67x$ ($r = 0.99$).

TABLE II

Quantification of Ca^{2+}-ATPase in basolateral membranes from porcine duodenum

100 μg pig ghost protein binds 267 cpm ^{125}I-calmodulin (Fig. 5). Pig ghost contains 1.73 ± 0.06 μg Ca^{2+}-ATPase/mg protein (Fig. 3B, $n = 3$). cpm ^{125}I-calmodulin bound to blots were determined in triplicate for each intestine. ATP-dependent ^{45}Ca uptake was measured for 1 min at 1 μM free Ca^{2+} (37 °C) and corrected for ATP-independent uptake. Values are the means ± S.E. with the number of experiments in parentheses. Control and rachitic animals are not significantly different. P values > 0.05.

	Control	Rachitic
^{125}I-calmodulin bound (cpm/50 μg protein)	426 ± 56 (5)	422 ± 50 (5)
Pig ghost equivalents/mg protein	3.2 ± 0.4	3.2 ± 0.4
μg Ca^{2+}-ATPase/mg protein	5.5 ± 0.7	5.5 ± 0.6
ATP-dependent ^{45}Ca uptake (nmol Ca^{2+}/mg protein per min)	2.6 ± 0.4 (5)	3.2 ± 0.4 (6)

ATPase for control and for rachitic piglets are presented in Table II. No differences between rachitic and control duodena were observed. The results of the competitive ELISA for sarcoplasmic reticulum Ca^{2+}-ATPase in the microsomal preparation are given in Table III, and again, there was no difference between control and rachitic animals.

ATP-dependent Ca^{2+} uptake

The ATP-dependent Ca^{2+} uptake in pig duodenal basolateral membrane vesicles is shown in Fig. 5. Addition of the Ca^{2+}-ionophore A23187 to vesicles which had reached steady-state Ca^{2+} uptake resulted in the release of accumulated ^{45}Ca. ATP-dependent Ca^{2+} uptake in pig intestinal microsomal membranes is stimulated in the presence of 20 mM oxalate (Fig. 6), which is typical for endoplasmic reticulum membranes [11,12,14]. The kinetics of ATP-dependent Ca^{2+} uptake in basolateral membranes were determined in three control and three rachitic duodena. The K_m values (mean ± S.E.) in control and rachitic preparations were 68 ± 15 and 55 ± 12 nM Ca^{2+}, respectively. The V_{max} values are given in Table II. In microsomal preparations, ATP-dependent Ca^{2+} uptake was mea-

TABLE III

Quantification of intracellular Ca^{2+}-ATPase in porcine duodenum

μg Ca^{2+}-ATPase/mg protein was measured as shown in Figs. 4A and B. ATP-dependent ^{45}Ca uptake was measured over 10 min at 37 °C in the presence of 20 mM oxalate and corrected for ATP-independent uptake. Values are the means ± S.E. with the number of experiments in parentheses. P values > 0.05.

	Control	Rachitic
μg Ca^{2+}-ATPase-mg protein	0.41 ± 0.02 (5)	0.36 ± 0.04 (5)
ATP-dependent ^{45}Ca uptake (nmol Ca^{2+} min per mg protein)	1.2 ± 0.2 (5)	1.4 ± 0.3 (4)

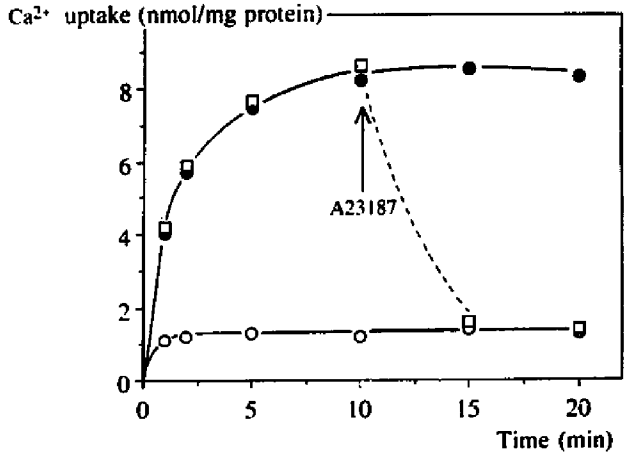

Fig. 5. ATP-dependent Ca^{2+} uptake in basolateral membranes from porcine duodenum. Time course of ^{45}Ca-uptake in the absence (●———●), and presence of ATP (○———○). (□———□; +ATP, +A23187 after 10 min.) ^{45}Ca uptake was measured at 1 μM free Ca^{2+} (37°C) (for further details see Methods).

sured in the presence of oxalate and the activities are given in Table III. There were no statistically significant differences in Ca^{2+} transport rates between control and rachitic preparations.

Discussion

To study effects of $1,25(OH)_2D_3$ on intestinal Ca^{2+}-absorption, vitamin D-deficient animals are required. So far, this has been achieved with rats or chicks raised on vitamin D-deficient diets, while being housed in dark rooms. The advantage of using piglets

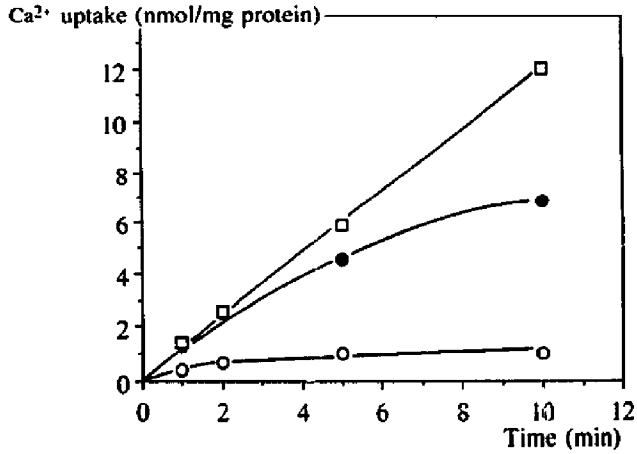

Fig. 6. ATP-dependent Ca^{2+} uptake in microsomes from porcine duodenum. Time course of ^{45}Ca-uptake in the presence of ATP + 0.1 mM vanadate (○———○), in the presence of ATP (●———●) and in the presence of ATP + 20 mM oxalate (□———□). ^{45}Ca uptake was measured at 1 μM free Ca^{2+} and 37°C. (For further details see Methods).

with pseudo vitamin D-deficiency rickets type I is that no special conditions are required to obtain rachitic controls, since the low levels of $1,25(OH)_2D_3$ are caused by lack of renal 1α-hydroxylase activity. Previously, Ghijsen and Van Os [22] showed that in vitamin D-deficient rats the activity of the plasma membrane Ca^{2+} pump was reduced. However, this reduction was not due to a lack of $1,25(OH)_2D_3$, but was shown to be induced by inactivation of Ca^{2+}-ATPase during enterocyte isolation procedures [23]. Differences in fatty acid composition in the sphingomyelin fraction of basolateral membranes, induced by vitamin D-deficient diets, were most likely responsible for this instability of the basolateral membrane Ca^{2+} pump [24]. In the present study, porcine duodenum proved a more convenient model, since enterocyte isolation procedures did not reduce basolateral membrane Ca^{2+} pump activity in $1,25(OH)_2D_3$-deficiency.

The present study confirms that vitamin D-deficiency does not affect Ca^{2+}-ATPase activities in duodenum when this activity is measured as the ATP-dependent ^{45}Ca uptake in basolateral membrane vesicles. However, using competitive ELISAs and ^{125}I-calmodulin binding, our work has now allowed the determination of the number of pump sites and has been able to show that pump density was not influenced by vitamin D-deficiency.

The present results imply that the efflux of Ca^{2+} across the basolateral membrane is not the rate-limiting step in transcellular Ca^{2+} transport. It is known, however, that $1,25(OH)_2D_3$ increases Ca^{2+} influx across the brush border and the amount of calbindin-D_{9K} in the cytosol [25]. Considering the high calbindin concentration in the duodenal enterocyte, it is anticipated that calbindin markedly enhances the diffusional flux of Ca^{2+} through the cytosol [25,26]. Consequently, in the presence of a sufficient pump capacity in the basolateral membrane, there would be no need to increase the number of Ca^{2+} pumps.

The present study allows the calculation of several parameters relevant to transcellular Ca^{2+} transport in the duodenum, such as the number of Ca^{2+} pump molecules per enterocyte, the turnover number of intestinal Ca^{2+}-ATPase and the maximum Ca^{2+} absorption rate per cm^2 of tissue. Assuming 10^8 cells/cm^2 in pig as in rat duodenum [27], of which roughly 50% are involved in active Ca^{2+} absorption since the lower villus and crypt regions do not absorb Ca^{2+} [4,25,28], and assuming that 1 cm^2 of pig duodenum equals 2 mg cell protein as in the rat [25], we calculate about $95 \cdot 10^3$ plasma membrane Ca^{2+} pump sites/enterocyte.

The turnover number for the basolateral Ca^{2+} pump can be calculated by combining the data in Table II. A V_{max} value of 3 nmol Ca^{2+}/min per mg in membrane vesicles of which only 15% are resealed inside-out

leads to a turnover number of roughly about 500 Ca^{2+} ions/pump site per min at 37°C. This is a factor of 2 lower than the turnover number reported for the red blood cell Ca^{2+}-ATPase [29]. From the pump density and the turnover number, we estimate that under V_{max} conditions the basolateral Ca^{2+} pump can remove Ca^{2+} from the cells with a rate of roughly about 500 nmol Ca^{2+}/h per cm^2 duodenum. Realizing that porcine duodenal transcellular Ca^{2+}-transport does not exceed 70 nmol Ca^{2+}/h per cm^2 (Kaune, unpublished observation), there is ample Ca^{2+} pump capacity to prevent the enterocyte from being flooded with Ca^{2+} entering the cells via the brush border membrane, under the influence of $1,25(OH)_2D_3$. Although the above calculations provide physiologically realistic values they are based on several assumptions, hence its uncertainty has to be acknowledged.

The competitive ELISA developed in this study for porcine erythrocyte Ca^{2+}-ATPase reached a similar sensitivity as the previously-reported competitive inhibition radioimmunoassay for purified human erythrocyte Ca^{2+}-ATPase [30]. The lack of immunological cross-reactivity of porcine intestinal Ca^{2+}-ATPase with anti-porcine erythrocyte Ca^{2+}-ATPase serum was unsurprising, since Verma et al. [30] had already demonstrated a weak cross-reactivity of rat and rabbit erythrocyte Ca^{2+}-ATPase with anti-human erythrocyte Ca^{2+}-ATPase. However, we have showed that the combination of a competitive ELISA and the ^{125}I-calmodulin overlay technique provides a sensitive assay for quantifying plasma membrane Ca^{2+}-ATPase in epithelial tissues. Recently, Borke et al. [31,32] described a monoclonal antibody, 5F10, raised against the human erythrocyte Ca^{2+} pump, which binds to a Ca^{2+} pump epitope in rat kidney and intestine. We have produced six monoclonal antibodies against porcine erythrocyte Ca^{2+}-ATPase, but no cross-reactivity with other tissues could be observed. The intracellular Ca^{2+}-ATPase in porcine duodenum exhibited a good cross-reactivity with anti-rat skeletal muscle sarcoplasmic reticulum Ca^{2+}-ATPase. This was anticipated since anti-rabbit SR Ca^{2+}-ATPase sera have been shown to exhibit good cross-reactivity with other tissues, even among different species [32,34]. The data in Table III demonstrate clearly that the Ca^{2+}-ATPase activity in enterocyte endoplasmic reticulum is of several orders of magnitude less than that in skeletal muscle cells [35]. There also appears to be more Ca^{2+}-ATPase activity in the plasma membrane than in intracellular membranes in porcine duodenal enterocytes, which is similar to the situation in rat enterocytes and rat kidney cortex [14].

In conclusion, we found that the vitamin D status of the animal is not reflected in Ca^{2+} pump capacities in the enterocyte. Therefore, the stimulatory effect of $1,25(OH)_2D_3$ on intestinal Ca^{2+} transport must be due to specific effects on brush border entry and on facilitation of Ca^{2+} diffusion, mediated by Ca^{2+}-binding proteins, through the cytosol.

Acknowledgements

We are indebted to Dr. H. Desmedt, Catholic University of Leuven, for providing us initially with ^{125}I-calmodulin; to Dr. J.A. Dempster for critical reading and improving English prose style, and to Mrs. S.E. Engels for editorial assistance.

References

1 Favus, J.M. (1985) Am. J. Physiol. 248, G147–G157.
2 Nellans, N.H. and Popovitch, J.E. (1981) J. Biol. Chem. 256, 9932–9936.
3 Ghijsen, W.E.J.M., De Jong, M.D. and Van Os, C.H. (1983) Biochim. Biophys. Acta 730, 85–94.
4 Van Corven, E.J.J.M., Roche, C. and Van Os, C.H. (1985) Biochim. Biophys. Acta 820, 274–282.
5 Ghijsen, W.E.J.M., Van Os, C.H., Heizmann, C.W. and Murer, H. (1986) Am. J. Physiol. 251, G223–G229.
6 Walters, J.R.F. and Weiser, M.M. (1987) Am. J. Physiol. 252, G170–G177).
7 Ghijsen, W.E.J.M. and Van Os, C.H. (1979) Nature 279, 802–803.
8 Ghijsen, W.E.J.M., De Jong, M.D. and Van Os, C.H. (1982) Biochim. Biophys. Acta 689, 327–336.
9 Moy, T.C., Walters, J.R.F. and Weiser, M.W. (1986) Biochem. Biophys. Res. Commun. 141, 979–985.
10 Van Corven, E.J.J.M., De Jong, M.D. and Van Os, C.H. (1986) Cell Calcium 7, 89–99.
11 Velasco, G., Shears, S.B., Michell, R.H. and Lazo, P.S. (1986) Biochem. Biophys. Res. Commun. 139, 612–618.
12 Van Corven, E.J.J.M., Verbost, P.M., De Jong, M.D. and Van Os, C.H. (1987) Cell Calcium 8, 197–206.
13 Ghishan, F.K. and Arab, N. (1988) Am. J. Physiol. 254, G74–G80.
14 Van Os, C.H., Van den Broek, L.A.M., Van Corven, E.J.J.M., Timmermans, J.A.H. and Dirven, H. (1988) Comp. Biochem. Physiol. 90A, 767–770.
15 Winkler, I., Schreiner, F. and Harmeyer, J. (1986) Calicif. Tissue Int. 38, 87–94.
16 Van Heeswijk, M.P.E., Geertsen, J.A.M. and Van Os, C.H. (1984) J. Membr. Biol. 79, 19–32.
17 Laemlli, U.K. (1970) Nature 227, 680–685.
18 Gopalakrishna, R. and Anderson, W.B. (1982) Biochem. Biophys. Res. Commun. 104, 830–836.
19 Bolton, A.E. and Hunter, W.M. (1973) Biochem. J. 133, 529–539.
20 Niggli, V., Adunyah, E.S., Penniston, J.T. and Carafoli, E. (1981) J. Biol. Chem. 256, 395–401.
21 Heilman, C. (1977) Eur. J. Biochem. 81, 211–222.
22 Ghijsen, W. and Van Os, C.H. (1982) Biochim. Biophys. Acta 689, 327–330.
23 Van Corven, E.J.J.M., De Jong, M.D. and Van Os, C.H. (1987) Endocrinology 120, 868–873.
24 Kaune, R., Van den Broek, L.A.M., Van Corven, E.J.J.M., De Grip, W.J. and Van Os, C.H. (1990) in Molecular and cellular regulation of calcium and phosphate metabolism (Peterlik, M. and Bronner, F., eds.), pp. 143–162, Alan R.Liss, New York.
25 Bronner, F., Pansu, D. and Stein, W.D. (1986) Am. J. Physiol. 250, G561–G569.
26 Feher, J.J. (1984) Biochim. Biophys. Acta 773, 91–98.
27 Harms, V. and Wright, E.M. (1980) J. Membr. Biol. 53, 119–128.
28 Van Os, C.H. (1987) Biochim. Biophys. Acta 906, 195–222.
29 Sarkadi, B. (1980) Biochim. Biophys. Acta 604, 159–190.

30 Verma, A.K., Gorski, J.P. and Penniston, J.T. (1982) Arch. Biochem. Biophys. 215, 345–354.
31 Borke, J.L., Minami, J., Verma, A.K., Penniston, J.T. and Kumar, R. (1987) J. Clin. Invest. 80, 1225–1231.
32 Borke, J.L., Caride, A., Verma, A.K., Penniston, J.T. and Kumar, R. (1990) Pflügers Arch. 417, 120–122.
33 Volpe, P., Krause, K.H., Hashimoto, S., Zorzato, F., Pozzan, T., Meldolesi, J. and Lew, D. (1988) Proc. Natl. Acad. Sci. USA 85, 1091–1095.
34 Hashimoto, S., Bruno, B., Lew, D.P., Pozzan, T., Volpe, P. and Meldolesi, J. (1989) J. Cell Biol. 107, 2523–2531.
35 Carafoli, E. (1987) Annu. Rev. Biochem. 56, 395–433.